# De Novo Design of a New Class of "Hard–Soft" Amorphous, Microphase-Separated, Polyolefin Block Copolymer Thermoplastic Elastomers

Kaitlyn E. Crawford and Lawrence R. Sita*

Department of Chemistry and Biochemistry, University of Maryland, College Park, Maryland 20742, United States

Ⓢ *Supporting Information*

ABSTRACT: Sequential cyclic/linear/cyclic living coordination polymerization of 1,6-heptadiene (HPD), propene, and HPD, respectively, employing the well-defined and soluble group 4 transition-metal initiator, $\{(\eta^5\text{-}C_5Me_5)Hf(Me)[N(Et)C(Me)N(Et)]\}[B(C_6F_5)_4]$, provides the stereo-irregular, amorphous poly(1,3-methylenecyclohexane)-*b*-atactic polypropene-*b*-poly(1,3-methylenecyclohexane) (PMCH-*b*-aPP-*b*-PMCH) polyolefin triblock copolymer (**I**) in excellent yield. By varying the weight fraction of the end group, minor component "hard" PMCH block domains, f_{PMCH}, relative to that of the midblock "soft" aPP domain, three different compositional grades of these polyolefin block copolymers, **Ia–c**, were prepared and shown by AFM and TEM to adopt microphase-separated morphologies in the solid state, with spherical and cylindrical morphologies being observed for f_{PMCH} = 0.09 (**Ia**) and 0.23 (**Ic**), respectively, and a third more complex morphology being observed for **Ib** (f_{PMCH} = 0.17). Tensile testing of **Ia–c** served to establish these materials as a new structural class of polyolefin thermoplastic elastomers, with **Ia** being associated with superior elastic recovery (94 ± 1%) after each of several stress–strain cycles.
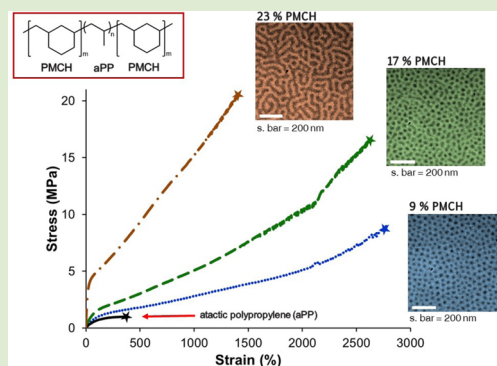
At the close of the 20th century, a "Holy Grail" of organometallic chemistry and polymer science was to achieve the living (stereoselective) coordination polymerization (LCP) of olefins.[1] Today, this goal has now been accomplished using several different classes of molecularly discrete transition-metal-based initiators.[2,3] However, the emergence of new fundamental forms of polyolefins that possess technologically useful physical properties has not been as quick to emerge with LCP as was once either imagined or expected.[2b] Indeed, a notable gap that still exists in the catalogue of polyolefins is the extreme rarity of examples of *direct* polyolefin block copolymers (BCPs) that arise as a product of sequential LCP of two or more different olefin monomers to form dissimilar types of covalently linked block domains.[4,5] BCPs represent a scientifically and technologically important class of polymer architecture by virtue of the ability of these materials to undergo spontaneous microphase separation of block domains to generate stable, long-range periodic nanostructures with features sizes on the order of 10–100 nm.[6] One of the most important archetypes for microphase-separated BCPs is provided by the family of amorphous polystyrene-*b*-polybutadiene (SB) copolymers that are prepared through the sequential living anionic polymerization of styrene and butadiene and which are now commonly referred to under the broader category of styrenic block copolymers (SBCs).[7] SBCs and, in particular, a SBS triblock architecture that is comprised of two polystyrene (S) end-group block domains that are coupled to a polybutadiene (B) midblock domain have

commercial value as thermoplastic elastomers (TPEs).[7,8] Within this SBS construct, the "hard" S domains are associated with a high glass transition temperature, T_g, of ca. 100 °C, while the "soft" B domains possess a low T_g value of <−40 °C. Importantly, as Scheme 1 presents, it is the microphase

Scheme 1
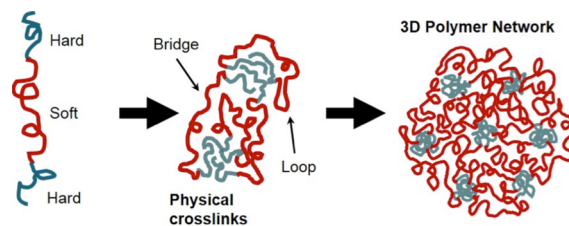
separation of this "hard–soft" block copolymer motif that is critically responsible for generating a 3D network of hard domains that serve as physical cross-links for restoring a TPE upon release of a strain-induced distortion.[8]

The challenges of applying the above set of well-established theories, or "first-principles", that have been developed for "hard–soft" amorphous microphase-separated BCPs for the

design of new structural classes of pure polyolefin TPEs are enormous.[9−11] To begin, as previously alluded to, one must identify two different olefin monomers that are each amenable to LCP but which together produce two different types of block domains that are immiscible with each other to the extent that microphase separation occurs in the absence of domain crystallization.[12] In addition, one of these monomers must be the progenitor of a minor, high T_g hard block domain that serves to form physical cross-links within a surrounding amorphous matrix of the major, low T_g soft block domain. Unfortunately, here, polyolefins as a class of materials have notoriously low T_g values in the absence of domain crystallinity. This latter property is not desirable in the present study since Register and co-workers[12] have shown that the "breakout" of crystallization within block domains can limit access to the full range of microphase-separated morphologies that are predicted for a completely amorphous BCP.[6] Herein, we now report the successful *de novo* design and experimental validation of a new family of "hard−soft" amorphous structurally well-defined direct polyolefin block copolymers from LCP that meet all the challenging criteria required for a microphase-separated BCP-based TPE. We further demonstrate the ability to fine-tune the morphology and elastic properties of these materials through simple adjustments to relative block domain lengths. With these results, the long-awaited potential of LCP of olefins is closer to being fulfilled.

We have previously reported that the LCP of ethene, propene, and longer-chain α-olefins can be achieved using a group 4 metal dimethyl, cyclopentadienyl, amidinate (CPAM) complex of general formula $Cp^*M[N(R^1)C(R^2)N(R^3)](Me)_2$ (M = Zr and Hf, $Cp^* = \eta^5$-C_5Me_5) (1) as the initiator after addition of a stoichiometric amount of the "activating" borate, $[PhNMe_2H][B(C_6F_5)_4]$ (2).[1e,3] We have also demonstrated that these same initiators can be used for the living cyclopolymerization of 1,5-hexadiene (HXD) and 1,6-hepta-diene (HPD) in chlorobenzene at subambient temperatures to produce poly(1,3-methylenecyclopentane) (PMCP) and poly-(1,3-methylenecyclohexane) (PMCH) polyolefins of tunable degrees of polymerization and narrow polydispersities.[5a,b] In the case of the C_1-symmetric preinitiator 1a (M = Zr, $R^1 = tert$-butyl, R^2 = Me, R^3 = Et), the LCP of HPD proceeds in a stereospecific manner to provide a crystalline, *cis*, isotactic-PMCH that is characterized by possessing both a high T_g value of 92 °C and a melting temperature, T_m, of 209 °C.[5b] On the other hand, when C_s-symmetric 1b (M = Hf, $R^1 = R^3$ = Et, R^2 = Me) is employed, stereoirregular, amorphous *cis*-PMCH (hereafter simply referred to as PMCH) is now obtained that is devoid of any crystallinity but which retains a desirable high T_g value of 72 °C. Finally, sequential LCP of 1-hexene followed by HPD using 1b and 2 for the initiator provided well-defined poly(1-hexene) (PH)-*b*-PMCH diblock BCPs that were shown to adopt a strongly microphase-separated cylindrical morphol-ogy in the case where the weight fraction of the PMCH block domain, f_{PMCH}, is 0.29 and the number-average molecular weight index, M_n, of the entire BCP is 28 kDa. Unfortunately, none of these PH-*b*-PMCH diblock materials displayed any significant level of elasticity in bulk samples.

Given the status of propylene as a readily available and sustainable commodity olefin monomer, it was decided that *atactic* polyproprene (aPP) would be more desirable than PH as an amorphous low T_g midblock that is sandwiched between two high T_g PMCH end-blocks. The LCP of both HPD and propene using the combination of 1b and 2 to provide the

corresponding PMCH and aPP homopolymers had previously been established by us. However, due to the different relative rates of propagation of these two monomers, it was not a given that well-defined PMCH-*b*-aPP-*b*-PMCH triblock copolymers could be obtained in living fashion, nor was it a given that such materials would adopt microphase-separated morphologies—or behave as TPEs for that matter. Thus, it was very gratifying to determine that three samples of the targeted PMCH-*b*-aPP-*b*-PMCH triblocks, Ia−c, could be synthesized with varying f_{PMCH} and M_n values according to Scheme 2 and Table 1.[13] A fourth sample of aPP that is similar in M_n value to the triblocks was also prepared as a control material for comparison purposes (see Table 1).
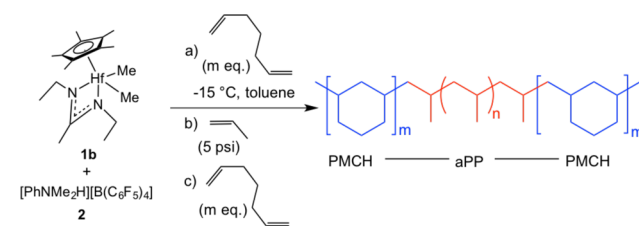
Scheme 2

Table 1. Molecular Weight, Polydispersity, and Tensile Test Data for PMCH-*b*-aPP-*b*-PMCH Triblock Copolymers, Ia−c, and aPP Homopolymer[13]

	$f_{PMCH}{}^a$	M_n (kDa)^b	$Đ^b$	stress (MPa)^c	strain (%)	rec. (%)^d
Ia	0.09	342	1.18	8.9	2773	94 ± 1
Ib	0.17	175	1.03	16.4	2631	93 ± 1
Ic	0.23	223	1.16	20.3	1390	72 ± 2
aPP	0	314	1.26	1.0	379	--

^{a}Calculated f_{PMCH} by determining the M_n (via GPC) of aliquots taken after complete polymerization of each segment compared to the overall M_n. ^{b}Determined by high-temperature gel permeation chromatography (HT-GPC). ^{c}Determined by stress−strain tensile testing. ^{d}Mean average of recovery % for ten consecutive cycles of applying and releasing a 300% strain on a freshly prepared sample (see Figure 1d).

An arsenal of analytical characterization tools were employed to establish that the PMCH-*b*-aPP-*b*-PMCH triblock materials Ia−c did indeed possess the well-defined block structure that was targeted. To begin, high-temperature gel permeation chromatography (HT-GPC) not only served to establish M_n and the weight-average molecular weight index, M_w, but also confirmed that the triblocks possessed narrow and monomodal molecular weight distributions as determined by the observed polydispersity index, $Đ$ (= M_w/M_n), values of <1.2.[3,13] High field ^{1}H (800 MHz) and ^{13}C (200 MHz) NMR spectroscopy conducted at 110 °C in 1,1,2,2-tetrachloroethane-d_2 further confirmed the integrity of the second and third block domains as being strictly aPP and PMCH homopolymers, respectively, rather than each of these blocks occurring as a random copolymer that arises from fortuitous insertion of a small amount of the previous comonomer used during construction of the next block segment.[13] Finally, while differential scanning calorimetry (DSC) of all three triblock samples displayed a characteristic low T_g phase transition at ca. 0 °C, as expected for the high molecular weight aPP midblock, it was not possible to observe the anticipated high T_g transition for the PMCH end-
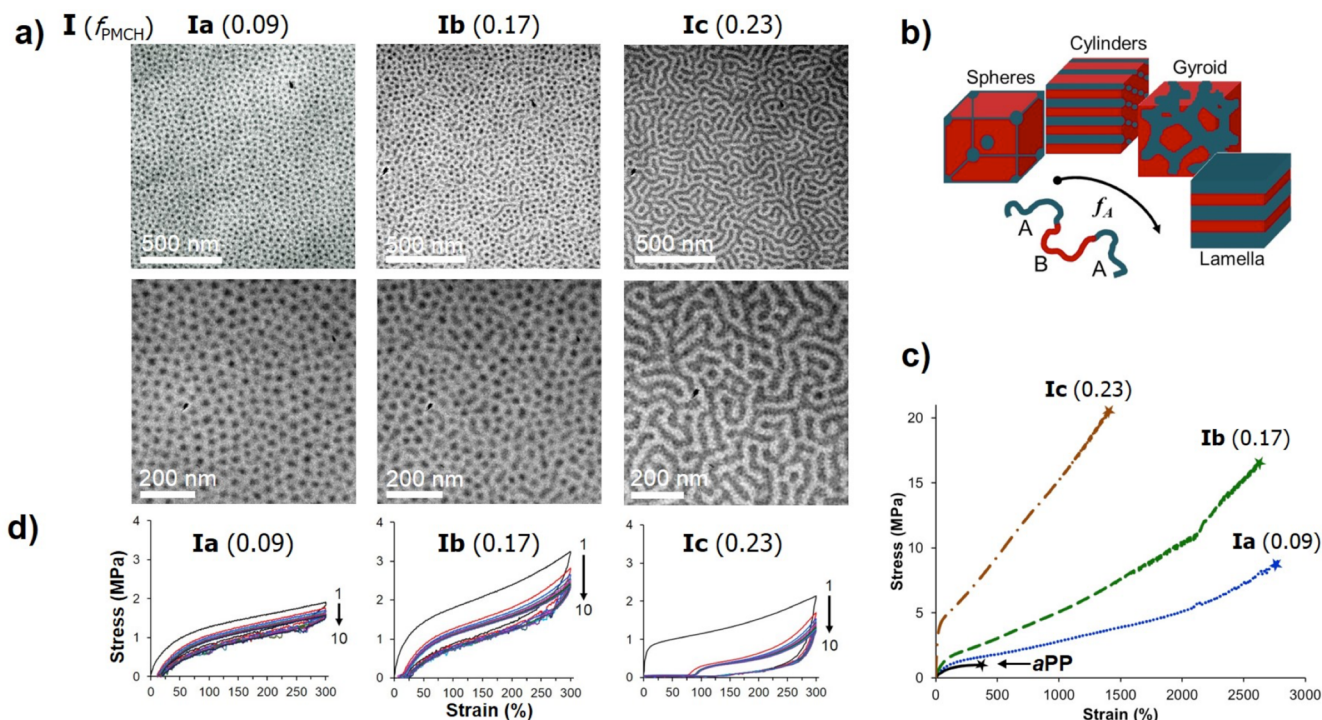
Figure 1. Clockwise: (a) TEM images (left to right, respectively) of **Ia–c** from Table 1 at two different magnifications (top and bottom). (b) Theoretical microphase-separated morphologies for BCPs as a function of the weight fraction of A block domain, f_A, in an ABA triblock copolymer. (c) Stress–strain curves for **Ia–c** and a aPP sample of similar molecular weight. (d) Repetitive stress–strain cycles (10 each) for **Ia–c**. First cycle is the black line for a fresh as-prepared sample.[13]

blocks by this analytical method. It is probable that the sensitivity of the DSC instrument was simply too low given the small relative f_{PMCH} and M_n values for the PMCH block segments in these particular PMCH-*b*-aPP-*b*-PMCH triblock materials (see Table 1).

As previously noted, synthesis of well-defined PMCH-*b*-aPP-*b*-PMCH triblock structures does not guarantee that these materials will undergo spontaneous microphase separation in the solid state and at temperatures that are relevant for potential applications. Accordingly, extensive characterization of the bulk structures of these triblock materials was conducted using phase-sensitive tapping mode (ps-tm) AFM, transmission electron microscopy (TEM), and small-angle X-ray scattering (SAXS) techniques.[14−17] Gratifyingly, as the data reproduced in Figure 1 show, the PMCH-*b*-aPP-*b*-PMCH samples indeed adopt microphase-separated morphologies within ultrathin films.[13] More specifically, phase-shift maps[5,13,14] obtained from ps-tm AFM analysis of ultrathin films (120−160 nm thick), supported on a crystalline silicon substrate and annealed under vacuum (0.1 mmHg) at 100 °C for 18 h, provided clear evidence of a microphase-separated morphology in each case (see Supporting Information). This conclusion was additionally confirmed through TEM analysis using similar ultrathin films of these materials supported on a 400-mesh carbon-coated copper grid and which yielded the (unstained) TEM images shown in Figure 1a.[13,15] Importantly, each triblock sample displayed a different microphase-separated morphology as a function of f_{PMCH} and degree of polymerization, N, in agreement with expectations based on a typical phase diagram governing the solid-state structures for a generic microphase-separated ABA triblock copolymer (see Figure 1b).[6] For **Ia** of Table 1 in which f_{PMCH} = 0.09, both ps-tm AFM (not shown)[13] and TEM images (see leftmost column of Figure 1a) support a solid-state

BCP structure that most closely approximates a slightly disordered body-centered cubic (BCC) array of PMCH spheres within an aPP matrix, with an average domain spacing of 50 nm. Likewise, sample **Ic** provided ps-tm AFM[13] and TEM data (see right most column of Figure 1a) that, based on the relatively small f_{PMCH} value of 0.23, are supportive of a cylindrical, rather than a lamellar, microphase-separated morphology in the solid state, with an average domain spacing of 50 nm. Finally, **Ib**, with a f_{PMCH} value of 0.17, curiously gave rise to ps-tm AFM[13] and TEM images for this PMCH-*b*-aPP-*b*-PMCH sample that revealed a more complex microphase-separated morphology as evidenced by a certain degree of continuity appearing between some PMCH domains (see middle column of Figure 1a). Unfortunately, attempts to obtain additional structural information through SAXS interrogation of melt-compressed films of the three PMCH-*b*-aPP-*b*-PMCH samples did not produce data from which any definitive conclusions regarding solid-state structure could be reached.[14,17]

It is has now been well established that, along with the relative weight fraction of the hard domain, there exists a strong correlation between the solid-state structure of a microphase-separated hard, soft ABA triblock-based TPE and its mechanical properties.[17] Given this knowledge base, it is possible to conduct a first-level analysis of stress−strain curves obtained for **Ia−c** through mechanical tensile testing of "as-prepared" dog-bone specimens that were die-cut from a melt-compressed 0.5 mm thick film (5 kpsi at 105 °C for 45 min followed by slow cooling) and elongated at a rate of 2 in./min until break.[13] To begin, as Figure 1c and Table 1 present, a steady increase in the ultimate tensile strength was observed for the PMCH-*b*-aPP-*b*-PMCH triblocks as the weight fraction of the hard PMCH domain fraction increased (cf. **Ia**: 8.9 MPa, f_{PMCH} = 0.09; **Ib**:

16.4 MPa, 0.17; **Ic**: 20.3 MPa, 0.23). Second, **Ia** proved to be the most elastic material of the three, with the longest elongation at break of 2773%, followed by **Ib** at 2631%, and then **Ic** at 1390%. This latter observation is consistent with the spherical morphology of **Ia** being more easily deformed due to a 3D array of isolated glassy hard domains that are surrounded by a rubbery matrix of the soft block (cf. Scheme 1). In contrast, the nonoriented cylindrical morphology of **Ic** serves to establish a more continuous glassy domain structure throughout the material (cf. Figure 1a), with the consequence that the initial strain deformation of this material proceeds with a higher Young's modulus and evidence of yielding that is absent in **Ia**. Not surprisingly, the mechanical behavior of the more complex structure of **Ib** was seen to fall between that of **Ia** and **Ic**, and all three materials exhibited superior elastic properties over a homopolymer of aPP of similar molecular weight (see Figure 1c).

As a final consideration, additional tensile test specimens of **Ia–c** were subjected to ten repetitive stress–strain cycles with a maximum of 300% strain, and the % recovery in specimen length was measured after removal of the strain for each cycle. As the data in Figure 1d and Table 1 reveal, after a small amount of presumed strain-induced annealing of the sample that occurs during the first stress–strain cycle, the microphase-separated morphologies of **Ia** and **Ib**, with spherical and complex geometries, respectively, displayed excellent and nearly identical elastic recoveries of 94 ± 1% and 93 ± 1%, respectively, in subsequent stress–strain cycles. In contrast, under identical conditions, the mechanical profile of **Ic** shows characteristic behavior associated with "stress softening" in which the initial stress–strain cycle proceeds with high modulus and yielding and, eventually, to breakup of the glassy hard domain cylindrical network. After relaxation, the second stress–strain cycle then occurs with a significantly lower modulus and with more rubbery character (see Figure 1d).[17d]

In summary, the first-principles design, synthesis, and experimental validation of a structurally well-defined amorphous polyolefin block copolymer that functions as a TPE as the result of a strongly segregated solid state nanostructure has been successfully achieved for the first time through the use of LCP. Moreover, the results of this study establish that both the solid-state structure and the mechanical properties of the PMCH-b-aPP-b-PMCH triblock system can be manipulated in programmed fashion through simple adjustments to relative block length and overall degree of polymerization.[6,17] Most importantly, however, the present demonstrated ability to apply first-principles developed for other classes of polymers helps to bring the long-sought rewards of LCP of olefins closer to reality for "precision" polyolefins that can contribute to meeting the future technological needs of society.

ASSOCIATED CONTENT

ⓢ Supporting Information

The Supporting Information is available free of charge on the ACS Publications website at DOI: 10.1021/acsmacro-lett.5b00447.

Additional experimental details for polymer synthesis and characterization (PDF)

AUTHOR INFORMATION

Corresponding Author

*E-mail: lsita@umd.edu.

Notes

The authors declare no competing financial interest.

REFERENCES

(1) (a) Doi, Y.; Suzuki, S.; Soga, K. *Macromolecules* **1986**, *19*, 2896–2900. (b) Scollard, J. D.; McConville, D. H. *J. Am. Chem. Soc.* **1996**, *118*, 10008–10009. (c) Baumann, R.; Davis, W. M.; Schrock, R. R. *J. Am. Chem. Soc.* **1997**, *119*, 3830–3831. (d) Killian, C. M.; Tempel, D. J.; Johnson, L. K.; Brookhart, M. *J. Am. Chem. Soc.* **1996**, *118*, 11664–11665. (e) Jayaratne, K. C.; Sita, L. R. *J. Am. Chem. Soc.* **2000**, *122*, 958–959. (f) Tshuva, E. Y.; Goldberg, I.; Kol, M. *J. Am. Chem. Soc.* **2000**, *122*, 10706–10707. (g) Tian, J.; Hustad, P. D.; Coates, G. W. *J. Am. Chem. Soc.* **2001**, *123*, 5134–5135.

(2) (a) Edson, J. B.; Domski, G. J.; Rose, J. M.; Bolig, A. D.; Brookhart, M.; Coates, G. W. In *Controlled and Living Polymerizations: From Mechanisms to Applications*; Mueller, A. H. E., Matyjaszewski, K., Eds.; Wiley-VCH: Weinheim, Germany, 2009. (b) Coates, G. W.; Hustad, P. D.; Reinartz, S. *Angew. Chem., Int. Ed.* **2002**, *41*, 2236–2257.

(3) Sita, L. R. *Angew. Chem., Int. Ed.* **2009**, *48*, 2464–2472.

(4) The term 'direct' is used here to signify that the polyolefin is derived from the metal-mediated coordination polymerization of an olefin, rather than from a postpolymerization modification of a polymer obtained through a different polymerization mechanism; see, for instance, poly(vinylcyclohexane) that is obtained through hydrogenation of polystyrene: (a) Gehlsen, M. D.; Bates, F. S. *Macromolecules* **1993**, *26*, 4122–4127. (b) Adams, J. L.; Quiram, D. J.; Graessley, W. W.; Register, R. A.; Marchand, G. R. *Macromolecules* **1998**, *31*, 201–204. (c) Lim, L. S.; Harada, T.; Hillmyer, M. A.; Bates, F. S. *Macromolecules* **2004**, *37*, 5847–5850.

(5) See, for instance: (a) Jayaratne, K. C.; Keaton, R. J.; Henningsen, D. A.; Sita, L. R. *J. Am. Chem. Soc.* **2000**, *122*, 10490–10491. (b) Crawford, K. E.; Sita, L. R. *J. Am. Chem. Soc.* **2013**, *135*, 8778–8781. (c) Crawford, K. E.; Sita, L. R. *ACS Macro Lett.* **2014**, *3*, 506–509.

(6) (a) Bates, F. S. *Science* **1991**, *251*, 898–905. (b) Hamley, I. W. *The Physics of Block Copolymers*; Oxford University Press: New York, 1999. (c) Hadjichristidis, N.; Pispas, S.; Floudas, G. *Block Copolymers Synthetic Strategies, Physical Properties, and Applications*; John Wiley & Sons, Inc.: NJ, 2003.

(7) (a) Gergen, W. P. In *Functional Polymers*; Bergbreiter, D. E., Martin, C. R., Eds.; Springer-Verlag: New York, 1989. (b) Scheirs, J.; Priddy, D. B. In *Modern Styrenic Polymers: Polystyrenes and Styrenic Copolymers*; Bening, R. C., Korcz, W. H., Handlin, D. L., Jr., Eds.; John Wiley & Sons: New York, 2003.

(8) Drobny, J. G. *Handbook of Thermoplastic Elastomers*; William Andrew Publications: New York, 2007.

(9) For examples of amorphous polyolefin BCPs prepared through LCP, see: (a) Gottfried, A. C.; Brookhart, M. *Macromolecules* **2003**, *36*, 3085–3100. (b) Leone, G.; Mauri, M.; Bertini, F.; Canetti, M.; Piovani, D.; Ricci, G. *Macromolecules* **2015**, *48*, 1304–1312. (c) Liu, W.; Zhang, X.; Bu, Z.; Wang, W.-J.; Fan, H.; Li, B.-G.; Zhu, S. *Polymer* **2015**, *72*, 118–124.

(10) A unique class of 'blocky' hard−soft amorphous poly(ethylene-*co*-octene) materials are known to undergo phase separation on a longer micron-length scale and have been commercialized by Dow Chemical as polyolefin-based TPEs, see: Arriola, D. J.; Carnahan, E. M.; Hustad, P. D.; Kuhlman, R. L.; Wenzel, T. T. *Science* **2006**, *312*, 714−719.

(11) Structurally well-defined, semicrystalline stereoblock polypropylene materials form a different class of polyolefin TPE in which the physical cross-links are established between crystalline stereoregular domains within a matrix of amorphous stereoirregular domains; see, for instance: (a) Busico, V. In *Stereoselective Polymerization with Singe-Site Catalysts*; Baugh, L. S., Canich, J. A. M., Eds.; CRC Press: Boca Raton, FL, 2008. (b) Harney, M. B.; Zhang, Y.; Sita, L. R. *Angew. Chem., Int. Ed.* **2006**, *45*, 2400−2404. (c) Giller, C.; Gururajan, G.; Wei, J.; Zhang, W.; Hwang, W.; Chase, D. B.; Rabolt, J. F.; Sita, L. R. *Macromolecules* **2011**, *44*, 471−482. (d) Hotta, A.; Cochran, E.; Ruokolainen, J.; Khanna, V.; Fredrickson, G. H.; Kramer, E. J.; Shin, Y.-W.; Shimizu, F.; Cherian, A. E.; Hustad, P. D.; Rose, J. M.; Coates, G. W. *Proc. Natl. Acad. Sci. U. S. A.* **2006**, *103*, 15327−15332.

(12) (a) Bishop, J. P.; Register, R. A. *Macromolecules* **2010**, *43*, 4954−4960. (b) Hatjopoulos, J. D.; Register, R. A. *Macromolecules* **2005**, *38*, 10320−10322. (c) Lee, H. H.; Register, R. A.; Hajduk, D.; Gruner, S. M. *Polym. Eng. Sci.* **1996**, *36*, 1414−1424. (d) Loo, Y.-L.; Register, R. A.; Ryan, A. J. *Phys. Rev. Lett.* **2000**, *84*, 4120−4123. (e) Myers, S. B.; Register, R. A. *Macromolecules* **2009**, *42*, 6665−6670. (f) Sebastian, J. M.; Graessley, W. W.; Register, R. A. *J. Rheol.* **2002**, *46*, 863−879.

(13) Experimental details are provided in the Supporting Information.

(14) (a) van Dijk, M. A.; van den Berg, R. *Macromolecules* **1995**, *28*, 6773−6778. (b) Stocker, W.; Beckmann, J.; Stadler, R.; Rabe, J. P. *Macromolecules* **1996**, *29*, 7502−7507. (c) Wang, D.; Nakajima, K.; Fujinami, S.; Shibasaki, Y.; Wang, J.-Q.; Nishi, T. *Polymer* **2012**, *53*, 1960−1965.

(15) Sawyer, L.; Grubb, D.; Meyers, G. F. *Polymer Microscopy*; Springer Science: New York, 2008.

(16) (a) Kinning, D. J.; Thomas, E. L. *Macromolecules* **1984**, *17*, 1712−1718. (b) Martin, W. J. *Concise Encyclopedia of the Structure of Materials*; Elsevier Science: University of Oxford: UK, 2006; pp 44−46.

(17) (a) Hiromichi, K.; Inoue, T.; Moritani, M.; Hashimoto, T. *Macromolecules* **1971**, *4*, 500−507. (b) Odell, J. A.; Keller, A. *Polym. Eng. Sci.* **1977**, *17*, 544−559. (c) Seguela, R.; Prud'homme, J. *Macromolecules* **1981**, *14*, 197−202. (d) Honeker, C. C.; Thomas, E. L. *Chem. Mater.* **1996**, *8*, 1702−1714. (e) Dair, B. J.; Honeker, C. C.; Alward, D. B.; Avgeropoulos, A.; Hadjichristidis, N.; Fetters, L. J.; Capel, M.; Thomas, E. L. *Macromolecules* **1999**, *32*, 8145−8152. (f) Stasiak, J.; Squires, A. M.; Castelletto, V.; Hamley, I. W.; Moggridge, G. D. *Macromolecules* **2009**, *42*, 5256−5265. (g) Orimo, Y.; Hotta, A. *Macromolecules* **2011**, *44*, 5310−5317. (h) Araki, Y.; Shimizu, D.; Hori, Y.; Nakatani, K.; Saito, H. *Polym. J.* **2013**, *45*, 1140−1145.